Theor. Appl. Climatol. (2009) 95: 53–68
DOI 10.1007/s00704-007-0375-4
Printed in The Netherlands

Theoretical and Applied Climatology

[1] Department of Geography and Resources Management, Institute of Space and Earth Information Science, The Chinese University of Hong Kong, Hong Kong, China
[2] Chinese Academy of Sciences, Nanjing Institute of Geography and Limnology, Nanjing, China
[3] Laboratory for Climate Studies, National Climate Center, China Meteorological Administration, Beijing, China
[4] Department of Geosciences, University of Oslo, Oslo, Norway
[5] Jiangsu Key Laboratory of Forestry Ecological Engineering, Nanjing Forestry University, Nanjing, China

Spatial and temporal variability of precipitation over China, 1951–2005

Q. Zhang[1,2,3], C.-Y. Xu[4], Z. Zhang[5], Y. D. Chen[1], C.-L. Liu[1]

With 10 Figures

Received 26 July 2007; Accepted 8 December 2007; Published online 11 April 2008

Summary

Annual, winter and summer precipitation records for the period 1951–2005 from 160 stations in China were analysed using the rotated empirical orthogonal function (REOF), the Mann–Kendall trend test and the Continuous Wavelet Transform (CTW) method. The REOF method was used to analyse the annual and seasonal variability of precipitation patterns over China, the Mann–Kendall method was used to detect the temporal trend of the rotated principal components time series, and the continuous wavelet method was used to explore the periodicity of precipitation changes. In general, six coherent regions across China are identified using the REOF method: north-east China; the middle and lower Yangtze River basin; the Haihe River and the Liaohe River; north-west China; the middle Yellow River and the South-east Rivers (rivers in south-east China). Continuous wavelet transform results indicate that the significant 2–4 year and 6–9 year bands are the major period components. Precipitation in China is uneven in space and time, and its complex temporal structure and spatial variations are different in each season. The Mann–Kendall test results show that, in general, the middle and the lower sections of the Yangtze River are dominated by increasing annual, summer and winter precipitation. Increasing annual precipitation can be observed in north-west China. Increasing summer precipitation is found in north-east China and the Pearl River basin, and the South-east Rivers are dominated by increasing winter precipitation. The availability of water as a resource is in close association with precipitation changes; therefore, this research will be helpful to watershed-based water resource managers in China.

Correspondence: Dr. Qiang Zhang, Department of Geography and Resource Management, The Chinese University of Hong Kong, Shatin, NT, Hong Kong, China, e-mail: qiangzhang@cuhk.edu.hk

1. Introduction

Climate change is being influenced heavily by the effects of greenhouse gases, which will alter the regional hydrological cycle and subsequently precipitation changes. The evidence for human-induced global warming is now ''unequivocal'', (IPCC, 2007: http://en.wikipedia.org/wiki/IPCC_Fourth_Assessment_Report). The tremendous importance of water in both society and nature underscores the necessity of understanding how changes in climate could affect regional water supplies (Xu and Singh 2004). Labat et al. (2004) indicated that present global warming has led to changes in the global hydrological cycle and to the increased magnitude of global and continental runoff. This global trend should be quantified at the regional scale where both in-

creasing and decreasing trends are identified. Since the change in water resources is different from region to region under the changing climate (e.g., Zhang et al. 2006a), climatic changes and possible impacts on global/regional water resources are receiving increasing focus from the scientific community (e.g., Loukas et al. 2002; Camilloni and Barros 2003; Labat et al. 2004). Booij (2005) studied the impact of climate change on floods in the River Meuse (western Europe) using spatially and temporally changed climate patterns and a hydrological model with three different spatial resolutions, to investigate the variability and uncertainty of impacts of climate changes on river floods obtained from simulations of the hydrological model. Many studies have shown that the impacts of climatic changes on global/regional water resources hinge on the influences of climatic changes on the spatial and temporal distribution of precipitation (e.g., Gao et al. 2007). Global warming will alter regional hydrological cycles, and these alterations are different from region to region, which makes further investigation of the spatial and temporal variability of precipitation under the changing climate critical (e.g., Domroes et al. 1998; Lana et al. 2001).

The spatial distribution and seasonal variation of precipitation in China have been discussed widely (e.g., Qian et al. 2002; Gemmer et al. 2004). Liu et al. (2005) examined the spatial and temporal variation in daily precipitation from 1960 to 2000 observed at 272 weather stations. Their results indicated that precipitation in China had increased by 2% over the study period. Seasonally, they found that precipitation had increased in winter and summer but decreased in spring and autumn for the same period. Chen et al. (1991) studied the climate variation in China during 1951–1989, indicating that most of China was dominated by decreased precipitation, especially in northern and north-western China. Zhai et al. (1999a) reported no significant trend in annual precipitation over China between 1951 and 1995. Zhai et al. (1999b) investigated changing trends in annual precipitation and annual extreme precipitation in China during 1951–1995, and found no significant trends in annual precipitation, and 1-day and 3-day maximum precipitation. Wang et al. (2004) showed an increasing trend in precipitation variation during the second half of the 20th century in western China, while a similar trend was not found in eastern China, where the 20- to 40-year periodicities were predominant in the precipitation variations. Ren et al. (2000) studied the trend in spatial patterns of rainfall in China during 1951–1996, showing an increasing trend in summer precipitation over the mid-lower reaches of the Yangtze River and a decreasing trend over the Yellow River basin, but almost no change in the high latitude areas. Zhai et al. (2005), investigated the trends in annual and seasonal total precipitation and in extreme daily precipitation for the year, summer, and winter half years using a daily precipitation dataset of 740 stations across China for the period 1951–2000. Their study showed that precipitation changes display different properties in terms of specific regions and seasons in China. In general, precipitation in summer and winter increased, while in spring and autumn it decreased. Precipitation in west and north-west China decreased before the 1980s and increased after the 1980s. However, some conclusions are in disagreement. The different conclusions, or even contradictions, reported in the aforementioned studies are caused by the differences in the time period of the data used in the analyses, since the temporal trends depend on the time period of the data series and in which part of the time series the outliers (most wet years) appear.

Uneven seasonal and spatial distributions of precipitation usually result in the uneven distribution of flood and drought occurrence. For example, in the summer of 1997, south China was flooded with excessive rainfall, while one of the most severe droughts on record occurred in north China (e.g., Huang et al. 2000). Furthermore, water resource management usually refers to river basins. Therefore, an investigation of the spatial and temporal variability of precipitation based on long precipitation series in China at the river basin scale will be useful for the management of fluvial systems and water resources in China.

Much attention (e.g., Zhai et al. 2005) has been focussed on the variability of summer- and winter-time precipitation due to the fact that more than 40% of the total annual precipitation falls in summer, and the winter usually has the least precipitation of all seasons. To partially redress this inbalance, this study has chosen to focus an annual precipitation as well as on summer and winter precipitation.

As mentioned above, previous studies are limited in their research scope and data used. The

spatial and temporal variability of precipitation in China needs to be re-examined with more robust methods for thorough research on trends, periodicity and spatial patterns. The objectives of the current research are: 1) to detect spatial patterns of the annual, summer and winter precipitation identified using the Rotated Empirical Orthogonal Function (REOF) method; 2) to explore the trends of major precipitation modes identified by REOF using the Mann–Kendall trend test and 3) to detect the periodicity features of precipitation over China using the Morlet Wavelet Transform method. This research will be helpful in furthering the understanding of the trends and periodicity of precipitation over China, and also in watershed-based water resource management.

2. Data and methods

2.1 Data

This study uses 160 rain gauge stations which have good quality, continuous data records for the period 1951–2005 (Gemmer et al. 2004). The 160 stations have been chosen for two reasons: (1) the main objective of the study is to examine the changing spatial and temporal patterns of precipitation in China rather than to provide a high resolution precipitation dataset. The quality, continuity, homogeneity and the length of data records are considered to be more important than the number of stations. (2) Quality control and homogeneity testing of the meteorological stations were performed by calculating the von Neumann ratio (N), the cumulative deviations ($Q/n^{0.5}$ and $R/n^{0.5}$), and the Bayesian procedures (U and A) (Buishand 1982; Gemmer et al. 2004). The quality control and homogeneity tests show that data from the 160 stations used in the current study are homogeneous at the >95% confidence level and are of good quality (Gemmer et al. 2004). The data are from the National Climatic Centre (NCCC) of the China Meteorological Administration (CMA). The locations of the stations are shown in Fig. 1.

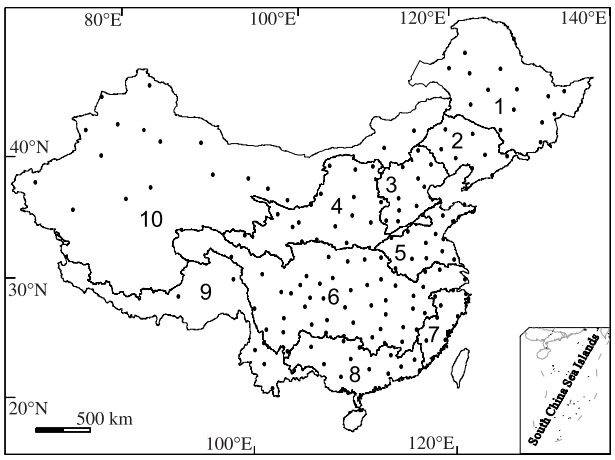

Fig. 1. Meteorological stations used in this study and the 10 drainage basins (after Gao et al. 2007, with minor revision). The solid dots denote the rain gauging stations. Numbers denote the 10 drainage basins: 1: SongHuajiang River; 2: Liaohe River; 3: Haihe River; 4: Yellow River; 5: Huaihe River; 6: Yangtze River; 7: SE Rivers (rivers in the southeast China); 8: Pearl River; 9: SW Rivers (rivers in the southwest China); 10: NW Rivers (rivers in the northwest China)

2.2 Methods

Principal Component Analysis is first applied to extract the general behaviour of all series to be analysed (Esteban-Parra et al. 1998). The empirical orthogonal function (EOF) analysis tends to identify physically and dynamically independent patterns (or normal modes) (Montroy 1997), which provide important clues as to the physics and dynamics of the system to be studied (e.g., Kim and Wu 1999). However, the physical interpretability of the obtained patterns is a matter of controversy because of the strong constraints satisfied by EOFs, namely orthogonality in both space and time. Physical modes such as normal modes (Simmons et al. 1983) are not, in general, orthogonal. This limitation has led to the development of the rotated empirical orthogonal function (REOF) (Richman 1986). Furthermore, REOF yields localised structures by compromising some of the EOF properties such as orthogonality. In a comparison study by Kim and Wu (1999), REOF was found to be good at dividing climatic patterns. In this paper, the varimax rotated empirical orthogonal function (REOF) method is used, meaning that the initial EOF modes are linearly transformed using the varimax method, which maximises the variance of the squared correlation coefficients between the time series of each REOF mode and each original EOF mode. The method increases the spatial variability of the obtained modes (Wang et al. 2006).

The trend in the rotated principal components (PC) time series has been analysed using the Mann–Kendall test. The non-parametric rank-

based Mann–Kendall method (MK) (Mann 1945; Kendall 1975) is commonly used to assess the significance of monotonic trends in hydro-meteorological time series (e.g., Helsel and Hirsch 1992; Zhang et al. 2006a, b). This test has the advantage of not assuming any distribution form for the data and is as powerful as its parametric competitors (Serrano et al. 1999). Therefore, it is recommended highly for general use by the World Meteorological Organization (Mitchell et al. 1966). In this study, the procedure of the Mann–Kendall test follows Gerstengarbe and

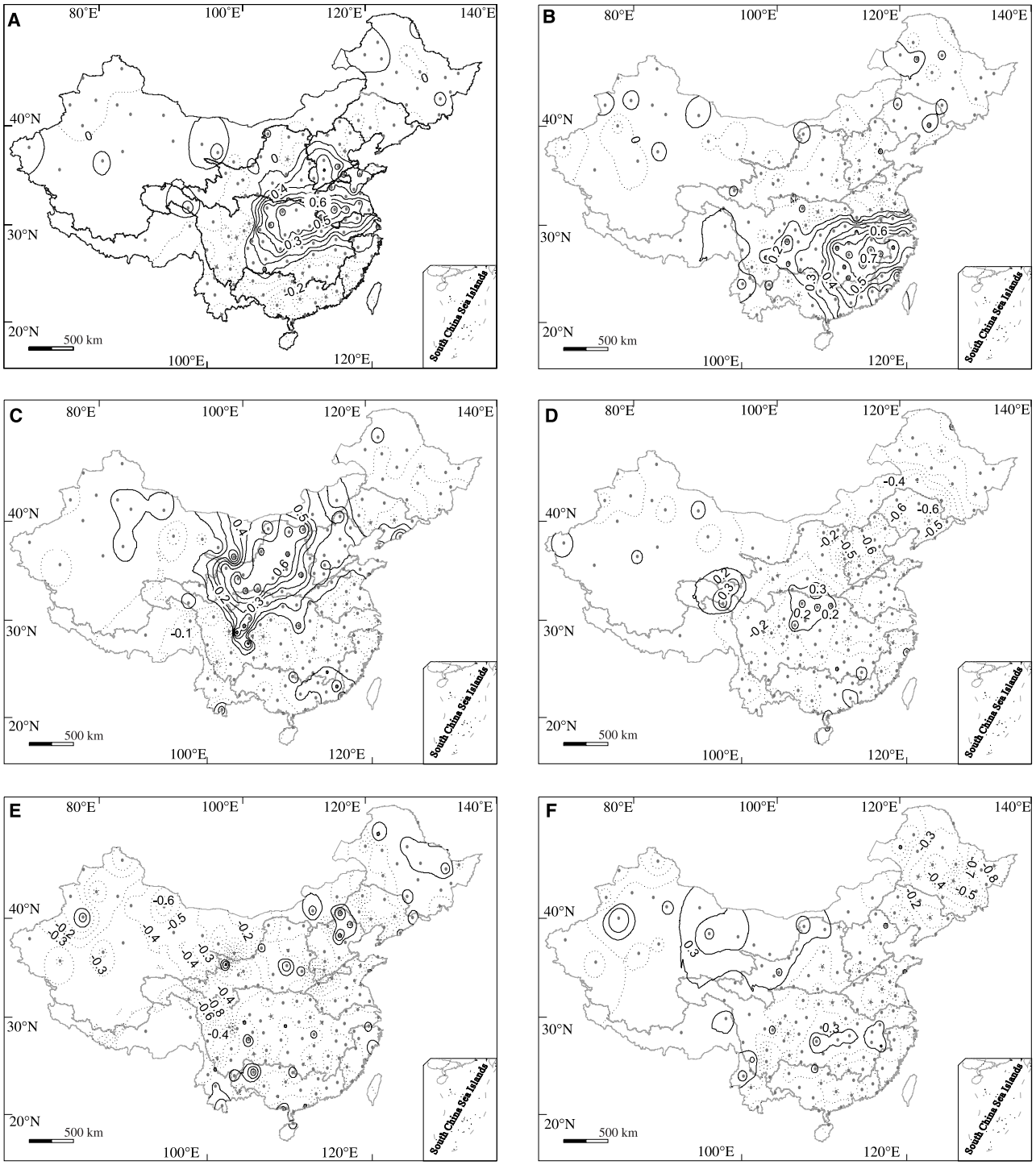

Fig. 2. Annual rotated REOF rainfall patterns for the period 1951–2005 for **A**: 1st REOF; **B**: 2nd REOF; **C**: 3rd REOF; **D**: 4th REOF; **E**: 5th REOF; **F**: 6th REOF

Werner (1999) who used the method to test an assumption regarding the beginning of the development of a trend within a sample $(x_1, x_2, \ldots, x_n)$ of the random variable X, based on the rank series r of the progressive and retrograde rows of this sample. The assumption (null hypothesis) is formulated as follows: the sample under investigation shows no start of a developing trend. In order to prove or to disprove the assumption, the following test is done. First a MK test statistic, d_k is calculated:

$$d_k = \sum_{i=1}^{k} r_i \quad (2 = k = n) \tag{1}$$

and

$$r_i = \begin{cases} +1 & \text{if } x_i > x_j \\ 0 & \text{otherwise} \end{cases} \quad (j = 1, 2, ..., i) \tag{2}$$

Under the null hypothesis of no trend, the statistic d_k follows a normal distribution with the expected value of $\mathrm{E}(d_k)$ and the variance $\mathrm{var}(d_k)$ as follows:

$$E[d_k] = \frac{n(n-1)}{4} \tag{3}$$

$$Var[d_k] = \frac{n(n-1)(2n+5)}{72} \tag{4}$$

Under the above assumption, the definition of the statistic index Z_k is calculated as:

$$Z_k = \frac{d_k - E[d_k]}{\sqrt{\mathrm{var}[d_k]}} \quad (k = 1, 2, 3, \ldots, n) \tag{5}$$

Z_k follows the standard normal distribution. In a two-sided test for trend, the null hypothesis is rejected at the significance level of α if $|Z| > Z_{(1-\alpha/2)}$, where $Z_{(1-\alpha/2)}$ is the critical value of the standard normal distribution with a probability exceeding $\alpha/2$. A positive Z value denotes a positive trend and a negative Z value denotes a negative trend. In this paper, the significance level of $\alpha = 5\%$ is used. In contrast to the traditional MK test which calculates the above statistic variables only once for the whole sample, the corresponding rank series for the so-called retrograde rows are similarly obtained for the retrograde sample $(x_n, x_{n-1}, \ldots, x_1)$. Following the same procedure as shown in Eqs. (1) to (5), the statistic variables, d_k, $E(d_k)$, $\mathrm{var}(d_k)$ and Z_k will be calculated for the retrograde sample. The Z values calculated with progressive and retrograde series are named Z_1 and Z_2, respectively, in this paper. The intersection point of the two lines, Z_1 and $Z_2 (k = 1, 2, \ldots, n)$ gives the point in time of the beginning of a developing trend within the time series. The null hypothesis (the sample is not affected by a trend) must be rejected if the intersection point is significant at the 5% level (i.e., outside the 95% confidence interval).

The influence of serial correlation in the time series on the results of the MK test has been discussed in the literature (e.g., von Storch 1995; Yue et al. 2002). In this study, before the MK test was applied, the meteorological series were tested for persistence using the serial correlation method (Haan 2002). Pre-whitening has been used to eliminate the influence of serial correlation (if significant) on the MK test (Yue and Wang 2004).

The current study uses the continuous wavelet transform (CWT) (Torrence and Compo 1998) method to study the periodicity of the PC series. We applied the Morlet wavelet in the current study because Morlet wavelet provides a good balance between time and frequency localisation. The wavelet is not completely localised in time. To ignore the edge effects, the Cone of Influence (COI) was introduced. Here, COI is the region of the wavelet spectrum in which edge effects become important and is defined here as the e-folding time for the autocorrelation of wavelet power at each scale. This e-folding time is chosen so that the wavelet power for a discontinuity at the edge drops by a factor e^{-2} and ensures that the edge effects are negligible beyond this point (Torrence and Compo 1998; Grinsted et al. 2004). The statistical significance of wavelet power can be assessed under the null hypothesis that the signal is generated by a stationary process, given the background power spectrum. A confidence

Table 1. Percentages of explained variance for each rotated EOF for the annual precipitation data

REOFs	Eigenvalue	Explained variance	Cumulated explained variance
1	16.8	11	11
2	14.1	9	2
3	12.7	8	28
4	9.8	6	34
5	8.6	5	39
6	7.6	5	44

level of 95% was taken as the threshold at which to classify the significance of the wavelet power. Detailed information of the continuous wavelet transform used in the current study was thoroughly introduced in Torrence and Compo (1998).

3. Results

3.1 Annual precipitation

Figure 2 demonstrates the annual precipitation patterns of the (varimax) rotated EOFs for China

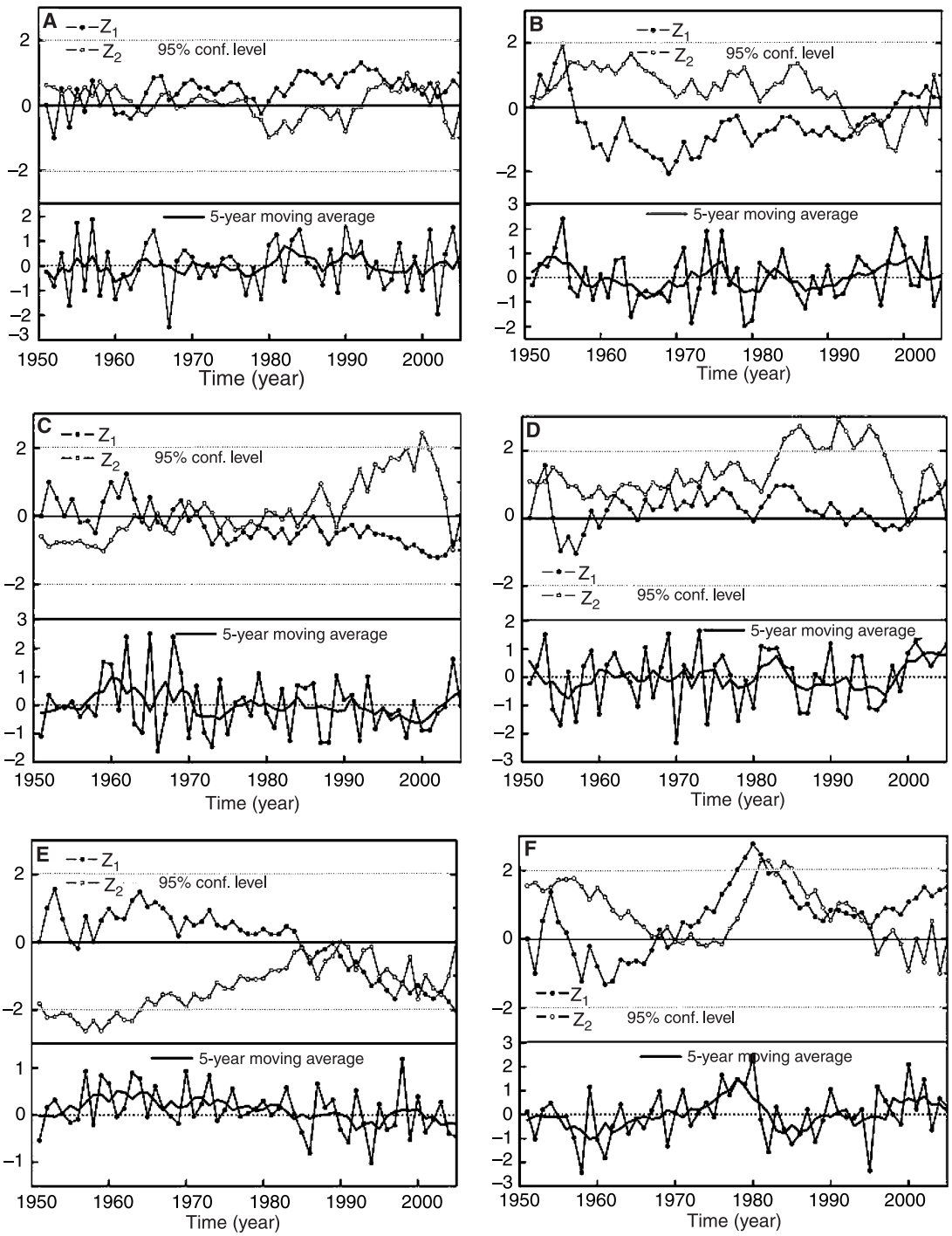

Fig. 3. Mann–Kendall trend of annual rotated PC series, rotated PC series and 5-year moving average (thick solid). Rotated PC series of **A**: 1st REOF; **B**: 2nd REOF; **C**: 3rd REOF; **D**: 4th REOF; **E**: 5th REOF; **F**: 6th REOF. The Z_1 and Z_2 are the MK statistic index. Positive Z value denotes increasing trend and *vice versa*. Detailed information about the Z_1 and Z_2 can be referred to Zhang et al. (2006a)

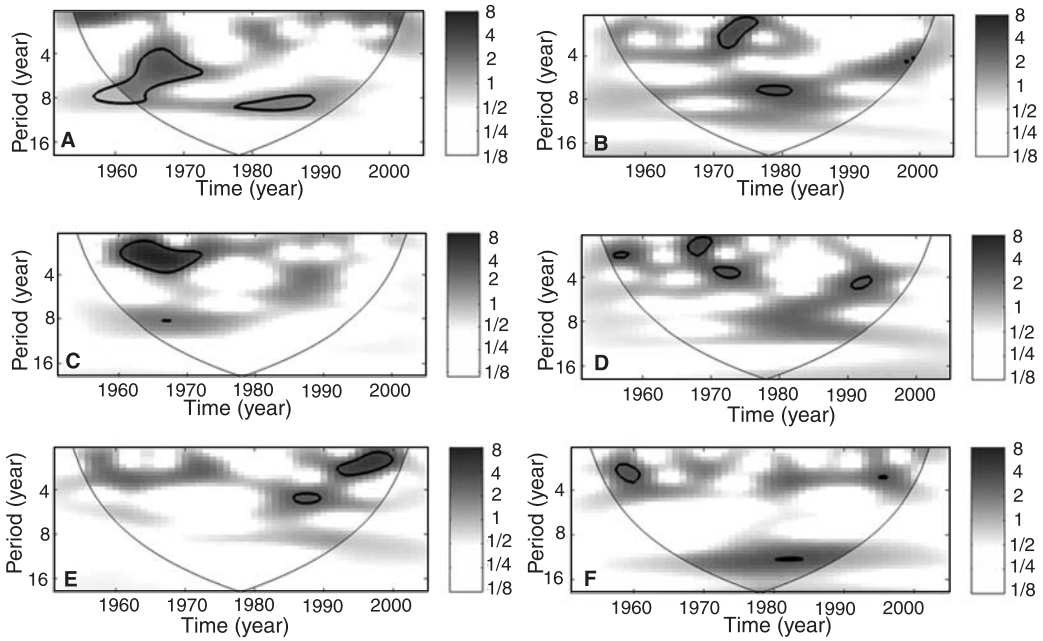

Fig. 4. Continuous wavelet transform of annual Rotated PC series of **A**: 1st REOF; **B**: 2nd REOF; **C**: 3rd REOF; **D**: 4th REOF; **E**: 5th REOF; **F**: 6th REOF. The thick black contour designates the 95% confidence level against red noise and the cone of influence (COI) where edge effects might distort the picture is shown as a lighter shade

by drawing the isolines of the loading factor values. Table 1 lists the percentage of variance explained by each REOF. The first REOF pattern (Fig. 2A) is centred mainly on the middle-north Yangtze River basin and middle-south Huaihe River basin. The MK trend test of the principal component (PC) time series of this region (Fig. 3A) indicates that precipitation increased after about 1962. However, no significant changing trend is detected at the >95% confidence level. The 5-year moving average identified no obvious dry or wet periods. The wavelet power spectra for the PCs are shown in Fig. 4A. The 95% confidence regions demonstrate that 1960–1970 and 1975–1990 include intervals of higher precipitation variance. Four to eight year periods are identified in precipitation series for 1960–1970 and a ∼8-year period for 1975–1990.

The second REOF pattern (Fig. 2B) dominates the south-east Yangtze River basin and the South-east Rivers (rivers in the southeast China). The precipitation of this region (Fig. 3B) decreased during 1951–1970 and increased thereafter. Wet periods are identified during 1951–1956, 1970–1978 and 1993–2005; dry periods, however, are detected during 1956–1970 and 1979–1993. Different periodicity features are shown in Fig. 4B compared to those of PCs of the first REOFs (Fig. 4A). Figure 4B indicates that the higher precipitation variance in the south-east Yangtze River basin and the South-east Rivers occurred around 1970 and 1980. These two periods have two significant year bands: 2–4 year band and 6–9 year band.

The middle Yellow River is associated with the 3rd REOF pattern (Fig. 2C), and the Liaohe River and the Haihe River are associated with the 4th REOF pattern (Fig. 2D). The MK trend indicates that the middle Yellow River basin is characterised by increasing precipitation during 1951–1969 and by decreasing precipitation during 1970–2000 (Fig. 3C). A 5-year moving aver-

Table 2. Percentages of explained variance for each rotated EOF for the summer precipitation data

REOFs	Eigenvalue	Explained variance	Cumulated explained variance
1	15.9	11	11
2	14.4	9	2
3	11.7	7	27
4	9.6	6	33
5	7.2	5	38
6	6.3	4	42

age also indicates a dry period during 1970–2000. The Liaohe River and the Haihe River basins are characterised by slightly decreasing precipitation (Fig. 3D) for the same period. The annual precipitation trend in the middle Yellow, Liaohe and Haihe Rivers is not significant at the >95% confidence level. These two regions have similar periodicity features, that is, the precipitation

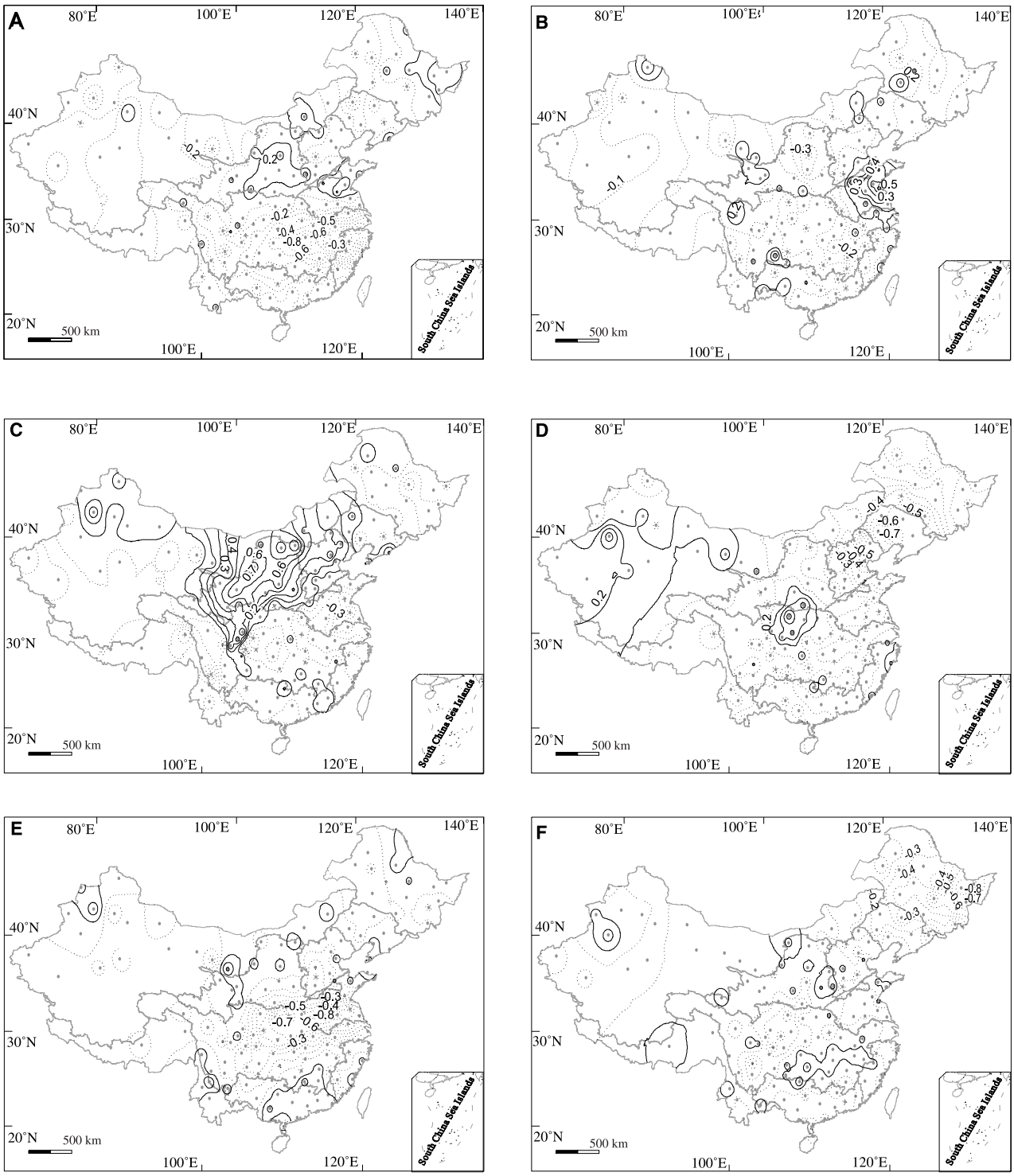

Fig. 5. Summer REOF rainfall patterns for the period 1951–2005 for **A**: 1st REOF; **B**: 2nd REOF; **C**: 3rd REOF; **D**: 4th REOF; **E**: 5th REOF; **F**: 6th REOF

changes are dominated by the shorter periods of the 2–4 year band, which is significant at the >95% confidence level. The higher precipitation variance occurred over the middle Yellow River in the 2–4 year band during 1960–1970 and for the Liaohe and Haihe Rivers in the 2–5 year band during ~1953, 1968–1975 and 1990–1993, respectively (see Fig. 4C, D).

Figure 2E illustrates that the 5th REOF is centred over the upper Yangtze River and the North-west Rivers (rivers in north-west China). North-east China is dominated by the 6th REOF

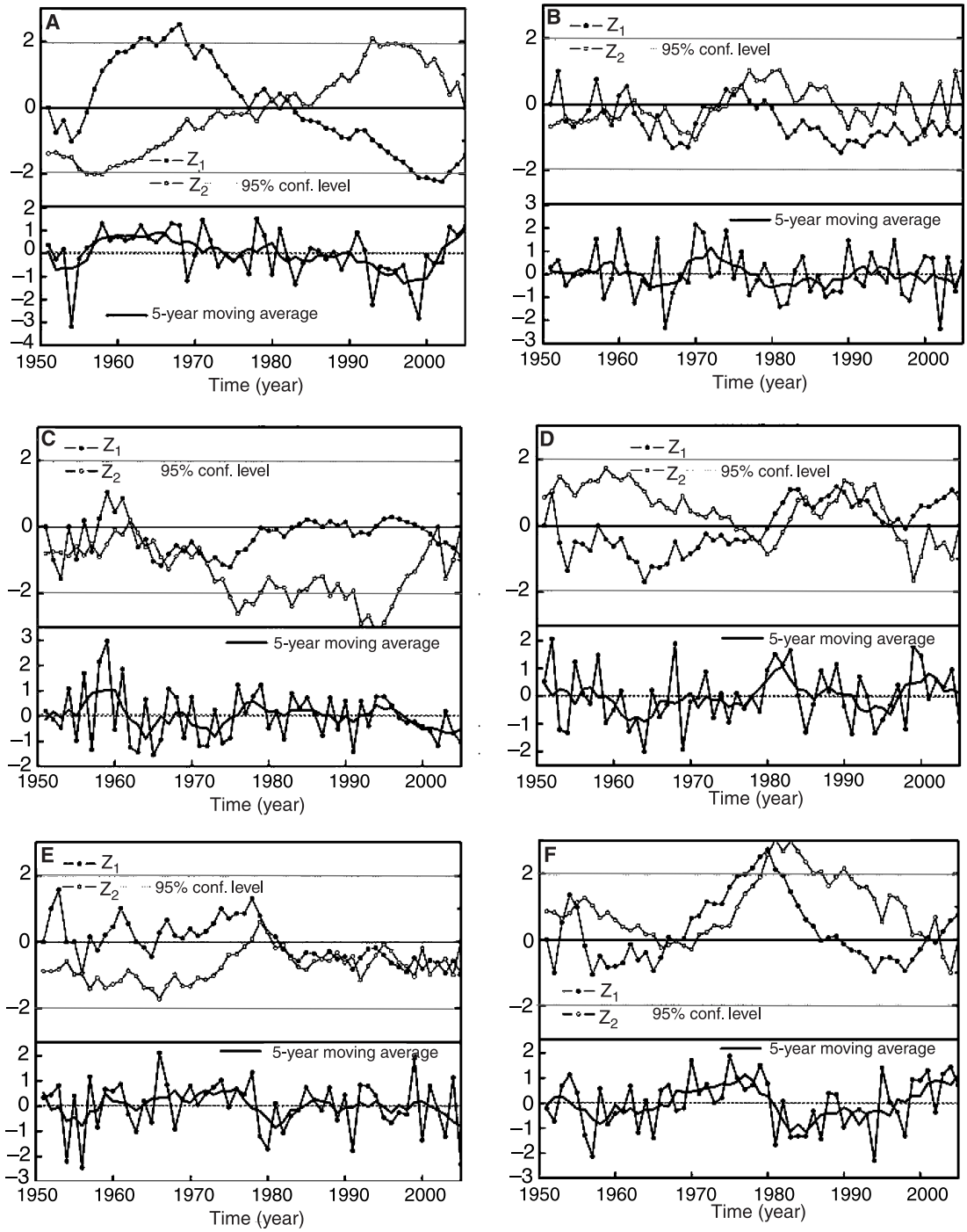

Fig. 6. Mann–Kendall trend of summer rotated PC series, rotated PC series and 5-year moving average (thick solid). Rotated PC series of **A**: 1st REOF; **B**: 2nd REOF; **C**: 3rd REOF; **D**: 4th REOF; **E**: 5th REOF; **F**: 6th REOF

(Fig. 2F). The loading factor values of these two REOF patterns are negative. The annual precipitation in north-west China has been decreasing since 1965 (Fig. 3E). The annual precipitation in north-east China is more variable with two periods dominated by increasing precipitation (1951–1960 and 1976–1985) and decreasing precipitation (1960–1975 and 1986–2005) (Fig. 3F). Wet periods are identified during 1955–1970 and 1981–1994; and dry periods are observed during 1970–1980 and 1995–2005. Higher precipitation variance occurred over north-west China during 1985–2000 in the 2–4 year band (Fig. 4E), and to north-east China during ∼1960 and 1980–1985 in the 2–4 and 10–15 year band, respectively.

3.2 Summer precipitation

Figure 5 shows the summer precipitation patterns of the (varimax) REOFs for China using the isolines of the loading factor values. Table 2 lists the percentage of variance explained by each REOF. The first and second REOFs (Fig. 5A, B) are associated alternatively with the precipitation regimes of the middle and lower Yangtze River and the Huaihe River. The summer precipitation in the middle and lower Yangtze River decreased during 1951–1968, but increased during 1968–2000. This increasing trend is significant at the >95% confidence level (Fig. 6A). The 5-year moving average also indicates a dry period during 1955–1980 and a wet period during 1980–2002. Huaihe River precipitation has decreased slightly, however, a relatively wet period has been identified with the 5-year moving average, i.e., 1969–1975 (Fig. 6B). The periodicity features of the precipitation series of the middle and lower Yangtze River and the Huaihe River are illustrated in Fig. 7A, B. Figure 7A indicates that the higher precipitation variance occurred during ∼1970 and ∼1980 in the 2–4 year band. The higher precipitation variance in the Huaihe River, however, occurred during 1958–1970 in the 5–7 year band (Fig. 7B).

The third REOF pattern is centred over the middle Yellow River and eastern part of the North-west Rivers (Fig. 5C). The fourth REOF pattern is associated with the precipitation regimes in the Liaohe and Haihe Rivers (Fig. 5D). The MK trend indicates no obvious increasing or decreasing precipitation changes in the middle Yellow River and eastern part of the North-west Rivers (Fig. 6C). Even so, two wet periods and two dry periods are also identified in Fig. 6C:

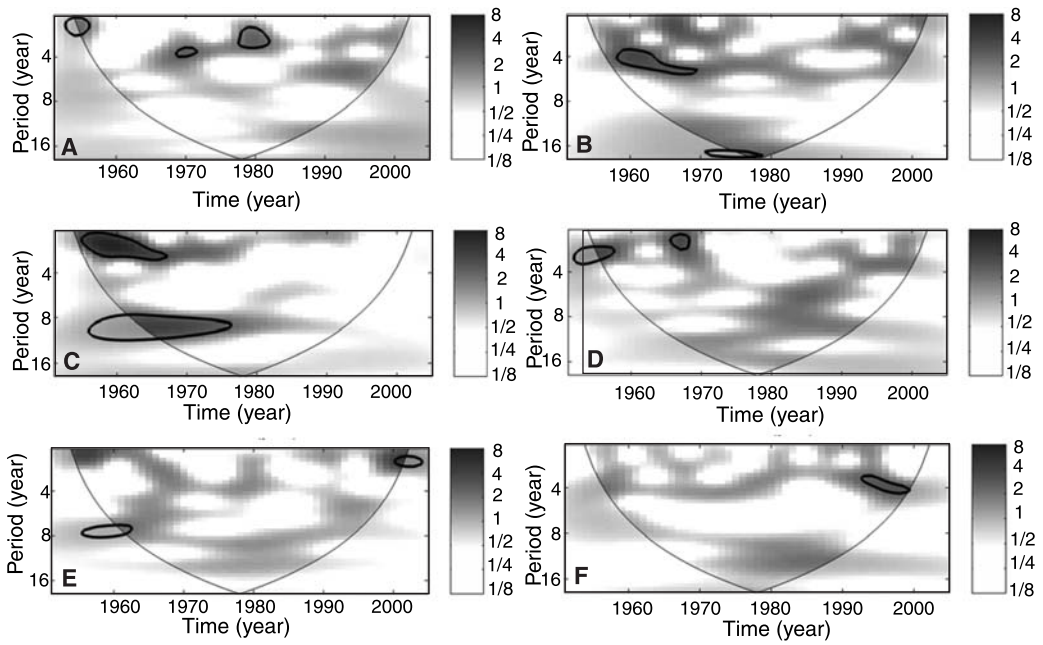

Fig. 7. Continuous wavelet transform of summer rotated PC series of **A**: 1st REOF; **B**: 2nd REOF; **C**: 3rd REOF; **D**: 4th REOF; **E**: 5th REOF; **F**: 6th REOF. The thick black contour designates the 95% confidence level against red noise and the cone of influence (COI) where edge effects might distort the picture is shown as a lighter shade

1951–1960 and 1975–1985 are relatively wet periods; 1960–1975 and 1986–2005 are relatively dry periods. A 5-year moving average also indicates decreasing summer precipitation during 1980–2005. It can be seen from Fig. 6D that the Liaohe and the Haihe Rivers are characterised by increasing precipitation during 1952–1964 and by decreasing precipitation during 1964–1983

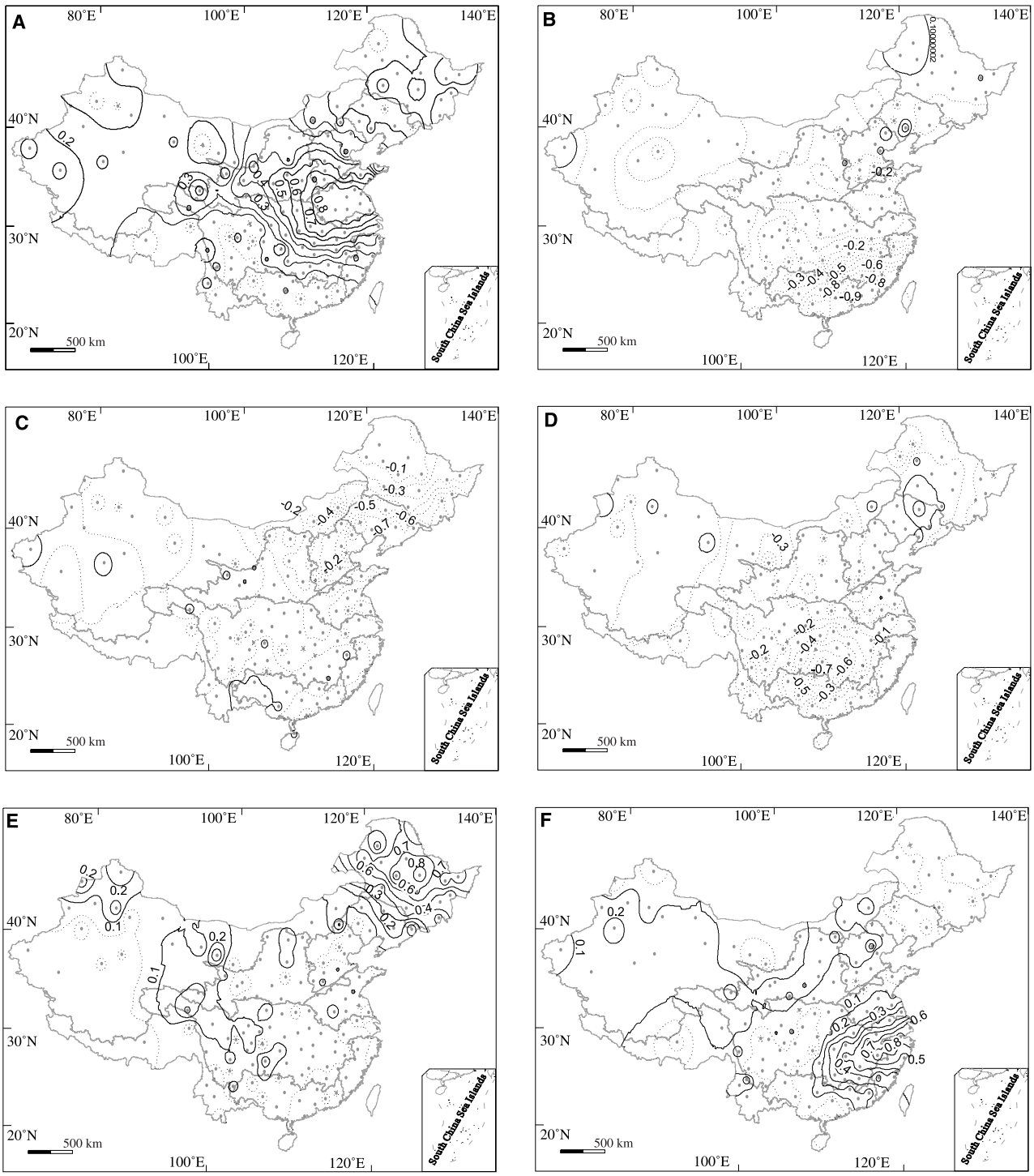

Fig. 8. Winter rotated EOF rainfall patterns for the period 1951–2005 for **A**: 1st REOF; **B**: 2nd REOF; **C**: 3rd REOF; **D**: 4th REOF; **E**: 5th REOF; **F**: 6th REOF

and 1995–2005. It can also be observed from Fig. 6D that 1980–1990 is characterised by dryness, and 1960–1975 by wetness. The periodicity features of the precipitation series of the regions are shown in Fig. 7C, D. The higher level of precipitation variance occurred to the 2–4 year band during 1955–1965 and the 8–10 year band during 1965–1975 for the third rotated pattern (Fig. 7C). The higher precipitation variance occurred to the 2–4 year band during 1965–1970 (Fig. 7D).

The fifth and sixth REOFs (Fig. 5E, F) are associated with the precipitation regimes in the Huaihe River, the north-middle Yangtze River and north-east China. MK trend test results indicate that the Huaihe River is characterised by decreasing precipitation during 1951–1978. Thereafter, increasing precipitation is detected in 1978 and 1980 (Fig. 6E). The summer precipitation in north-east China decreased during 1955–1980 and during 1985–2005, and increased during 1980–1985. Dry periods are identified during 1970–1980, and wet periods are identified during 1956–1965 and 1980–1998 (Fig. 6F). It can be seen from Fig. 7E that no significant periods are detected with the help of continuous wavelet transform method, which is different from the periodicity features of other PCs. As for the periodicity of precipitation in north-east China, higher precipitation variance occurred in the period 1990–2000 in the 3–5 year band.

3.3 Winter precipitation

Figure 8 demonstrates the winter precipitation patterns of the (varimax) REOFs over China by the isolines of the loading factor values. Table 3 lists the percentage of variance explained by each

Table 3. Percentages of explained variance for each REOF for the winter precipitation data

REOFs	Eigenvalue	Explained variance	Cumulated explained variance
1	34.8	22	22
2	20.1	13	35
3	10.7	7	42
4	9.1	6	48
5	7.3	5	53
6	5.6	4	57

REOF. The first REOF (Fig. 8A) is associated with the winter precipitation regimes of the middle Yangtze River basin, the Huaihe River and the lower Yellow River, and the second REOF centres on the Pearl River and in the south Yangtze River (Fig. 8B). It can be seen from Fig. 9a that no obvious changing patterns can be identified in the winter precipitation series from the middle Yangtze River, the Huaihe River and the lower Yellow River. A 5-year moving average shows three wet periods, i.e., 1970–1975, 1988–1993 and 2000–2002. In the Pearl River and the south Yangtze River (Fig. 9B), a 5-year moving average shows a wetter winter period during 1980–2000 and a dry winter period during 1960–1980. No periodicity features of the winter precipitation series can be detected in the middle Yangtze River basin, the Huaihe River and the lower Yellow River (Fig. 10A). The significant wavelet power can be found in the 2–3 and 6–8 year band around 1980–1985 and 1980–1990 in the Pearl River and the south Yangtze River (Fig. 10B).

The third REOF is centred on the Liaohe River and the Haihe River (Fig. 8C). The fourth REOF is dominant in the middle and south Yangtze River and the west Pearl River (Fig. 8D). The MK trend test result indicates that winter precipitation decreased after 1980 and no obvious wet or dry periods are identified in the Liaohe and Haihe Rivers (Fig. 9C). Figure 9D indicates that winter precipitation in the middle and the south Yangtze River and the west Pearl River decreased during 1960–1980 and increased thereafter until 1990. A relatively wet period during 1963–1979 and a relatively dry period during 1989–1998 have been identified by a 5-year moving average (Fig. 9D). Figure 10C demonstrates the significant wavelet power of winter precipitation in the 2–4 year band around 1990, and in the 6–9 year band during 1970–1990. No significant wavelet power is identified in winter precipitation in the middle and south Yangtze River and in the west Pearl River (Fig. 10D).

The fifth and the sixth REOFs (Fig. 8E, F) are associated with the winter precipitation regimes of north-east China, the lower Yangtze River and in the South-east Rivers. Figure 9E indicates that winter precipitation in north-east China decreased during 1955–1975 and increased during 1951–

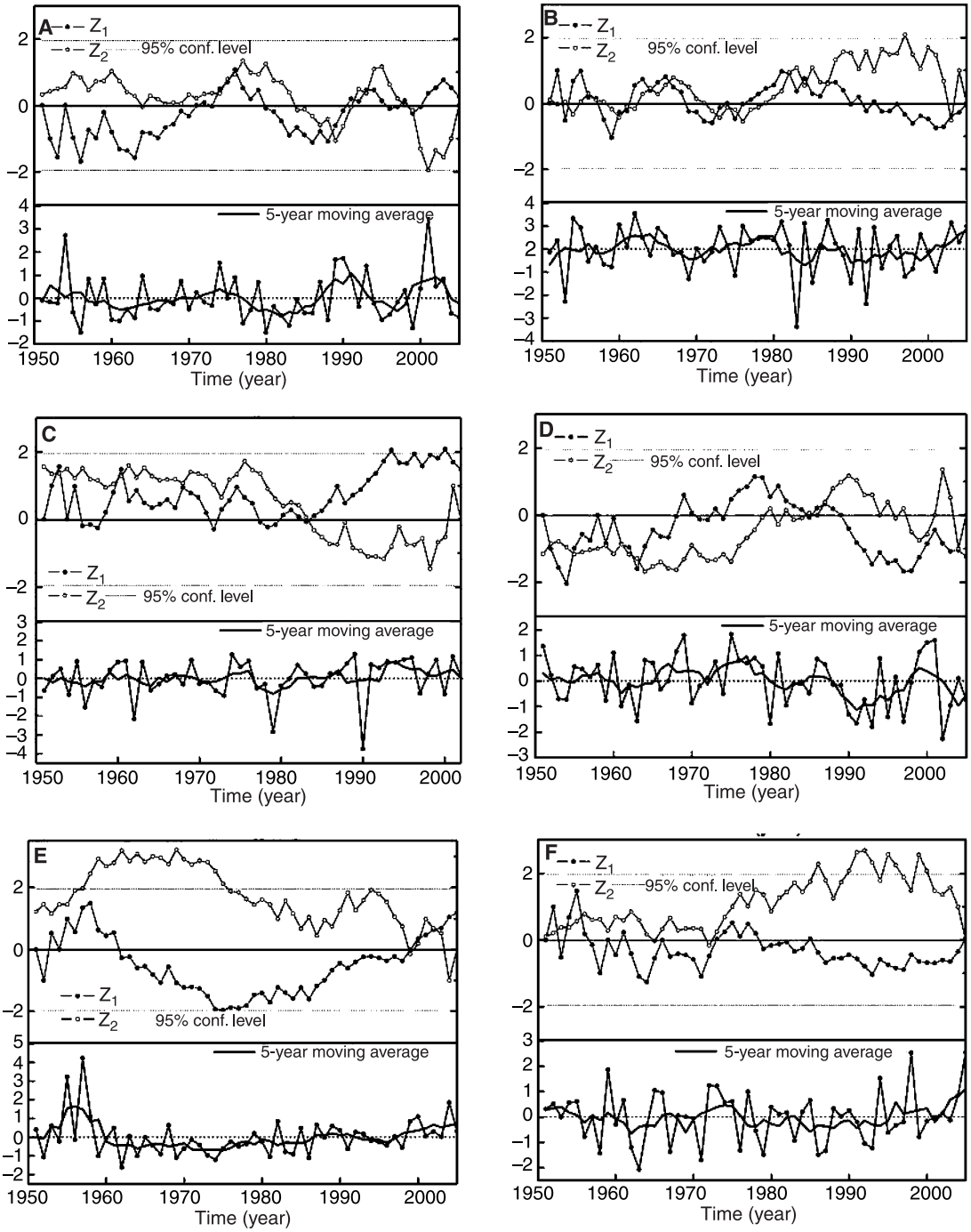

Fig. 9. Mann–Kendall trend of winter rotated PC series, rotated PC series and 5-year moving average (thick solid). Rotated PC series of **A**: 1st REOF; **B**: 2nd REOF; **C**: 3rd REOF; **D**: 4th REOF; **E**: 5th REOF; **F**: 6th REOF

1955 and 1975–2005. A 5-year moving average identifies a dry period during 1960–1990, and wet periods during 1951–1960 and 1999–2005. Winter precipitation in the lower Yangtze River and the South-east Rivers increased during 1988–2005, no obvious wet/dry periods are identified with a 5-year moving average (Fig. 9F). Continuous wavelet transform results indicate significant wavelet power in the 2–4 years band during 1955–1963 in north-east China (Fig. 10E), and in the 4–8 year band during 1960–1970 and in the 3–4 year band during 1995–1998 in the lower Yangtze River and the South-east Rivers (Fig. 10F).

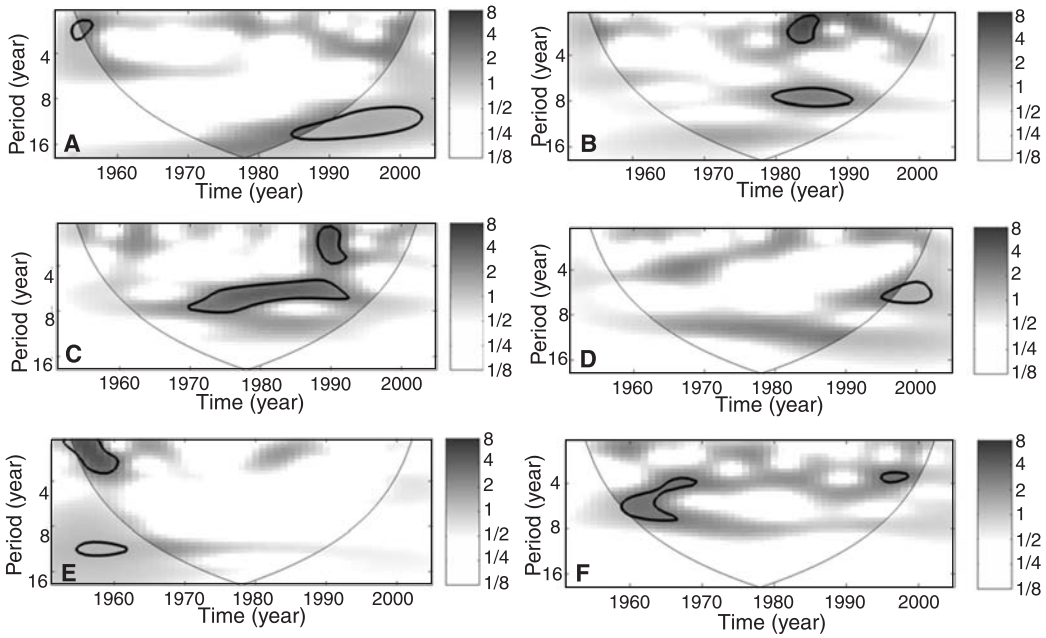

Fig. 10. Continuous wavelet transform of winter rotated PC series of **A**: 1st REOF; **B**: 2nd REOF; **C**: 3rd REOF; **D**: 4th REOF; **E**: 5th REOF; **F**: 6th REOF. The thick black contour designates the 95% confidence level against red noise and the cone of influence (COI) where edge effects might distort the picture is shown as a lighter shade

4. Conclusion and discussion

As shown in Sect. 3, no individual method can reveal the different statistical properties of precipitation variability, and each method has its own strength and weakness. The results of the three methods complement each other. Long series of the annual, winter and summer precipitation data for 1951–2005 from 160 stations in China were analysed using the rotated empirical orthogonal function (REOF) method, Mann–Kendall method, and continuous wavelet transform (CWT) method. The coherent regions of China vary with season as defined by annual, winter and summer time series. In general, six coherent regions in China are identified based on the REOF method: north-east China, the middle and lower Yangtze River basin, the Haihe River and the Liaohe River, the north-west China, the middle Yellow River, and the Sourth-east Rivers.

Precipitation in China presents a complicated spatial and temporal structure. It is uneven in space and time and this complex spatial and temporal structure is different in different seasons. In reality, several factors such as sea surface temperatures and Tibetan Plateau heating (Zhang et al. 2007) exert a tremendous influence on spatial and temporal precipitation changes over China. All these factors combine to result in the complex spatial and temporal structure of precipitation changes over China. Research results of the current study suggest that different change patterns occurred over the different regions of China for different seasons. For annual precipitation, north-east China is dominated by decreasing precipitation, especially after 1970. Decreasing precipitation also occurred over the middle and lower Yellow River and over the Huaihe River. Annual precipitation in the middle and lower Yangtze River and in the South-east Rivers has been increasing. North-west China is dominated by significant increasing precipitation after ∼1970. The start time of this increase is similar, namely, ∼1970. The precipitation in the Haihe and Liaohe River exhibits no obvious changing patterns.

Summer precipitation in north-east China has been decreasing since after ∼1980. The middle Yellow River and Huaihe River are dominated by decreasing precipitation. The South-east Rivers and north-west China are characterised by increasing precipitation after ∼1980. Summer precipitation in the middle and lower Yangtze River increased significantly during 1968–2005 and increased slightly over the Haihe and Liaohe Rivers. Almost all these changes have a similar start time of ∼1980–1985. In north-east China, annual precipitation has decreased since 1986; however, summer precipitation has increased since 1980. The interesting results are that winter precipitation

has increased over the middle and lower Yellow River and Huaihe River, and that these places are characterised by decreased summer precipitation. North-west China, the Haihe and Liaohe Rivers, the South-east Rivers and the Pearl River are dominated by increasing winter precipitation after about ∼1980, ∼1990, respectively. Increasing summer precipitation is found in north-east China. The Pearl River basin and the South-east Rivers are dominated by increasing winter precipitation.

The results of this research demonstrate that winter precipitation has increased and that summer and annual precipitation has decreased in some places in China, e.g., the middle and lower Yellow River and north-east China, respectively. Increasing precipitation is identified in north-west China. Zhai et al. (2005) and Gong and Ho (2002) also indicated significant positive trends in winter precipitation over Tibet, and significant increasing summer precipitation in the lower Yangtze River. Continuous wavelet transform results indicate that the periods of all the PCs share the similarly significant 2–4 year and ∼8 year periods. The climatic changes in China are controlled mainly by the winter and summer monsoon (Domroes and Peng 1988). In general, precipitation in south-west China is greater than in north-west China, and these precipitation patterns are determined mainly by the monsoon system and effects of topography (Zhai et al. 2005). Rainy seasons in eastern China depend on the progress and retreat of the East Asian summer monsoon. Detailed information on the evolution of the summer Asian monsoon and the associated propagation of the rain belt can be found in Ding (1994). In general, the rain belt propagates northward in early May and June and reaches north China between 5–25 August. After midsummer, the rain belt retreats southward rapidly, which directly determines precipitation changes across China. The MK trend test indicates a crossover of annual and seasonal precipitation changes during the 1970s and 1980s. These results suggest that change in precipitation are attributed to changes in the East Asian summer monsoon system. Wang (2001) indicated that the weakening of the Asian monsoon circulation after the 1970s is not beneficial for the northward propagation of the rain belt. Some Chinese scholars attributed precipitation anomalies to sea surface temperature anomalies in the equatorial eastern Pacific, the sub-tropical high across the north-west Pacific, the monsoon system and snow cover over Tibet in winter (e.g., Gong and Ho 2002; Zhao and Xu 2002). These studies indicate that various, complex influencing factors are responsible for changes in precipitation in China. The availability of water is closely associated with precipitation changes; therefore, this research will be helpful for watershed-based water resource management in China.

Acknowledgement

This research was supported financially by the Laboratory for Climate Studies, National Climate Center, China Meteorological Administration, China (Grant No: CCSF2007-35), the National Natural Science Foundation of China (Grant No.: 40701015), the Outstanding Oversea Chinese Scholars Fund from the Chinese Academy of Sciences and by the Direct Grant from the Faculty of Social Science, The Chinese University of Hong Kong (Project No. 4450183). Wavelet software was provided by C. Torrence and G. Compo, and is available from: http://paos.colorado.edu/research/wavelets/. Cordial thanks are extended to the two anonymous reviewers and the managing editor of theorectical and Applied Climatology, Prof. Dr. Hartmut Grassl, for their invaluable comments which improved greatly the quality of this paper.

References

Booij MJ (2005) Impact of climate change on river flooding assessed with different spatial model resolutions. J Hydrol 303: 176–198

Buishand TA (1982) Some methods for testing the homogeneity of rainfall records. J Hydrol 58: 11–27

Camilloni IA, Barros VR (2003) Extreme discharge events in the Paraná River and their climate forcing. J Hydrol 278: 94–106

Chen LX, Shao YN, Dong M, Ren ZH, Tian GS (1991) Preliminary analysis of climatic variation during the last 39 years in China. Adv Atmos Sci 8: 279–288

Ding Y (1994) Monsoons over China. Kluwer Academic Publishers, Dordrecht, 419 pp

Domroes M, Peng G (1988) The climate of China. Springer, Berlin Heidelberg New York, 361 pp

Domroes M, Kaviani M, Schaefer D (1998) An analysis of regional and intra-annual precipitation variability over Iran using multivariate statistical methods. Theor Appl Climatol 61: 151–159

Esteban-Parra JM, Rodrigo FS, Castro-Diez Y (1998) Spatial and temporal patterns of precipitation in Spain for the period 1880–1992. Int J Climatol 18: 1557–1574

Gao G, Chen DL, Xu C-Y, Simelton E (2007) Trend of estimated actual evapotranspiration over China during 1960–2002. J Geophys Res – Atmosph 112: D11120, doi: 10.1029/2006JD008010

Gemmer M, Becker S, Jiang T (2004) Observed monthly precipitation trends in China 1951–2002. Theor Appl Climatol 77: 39–45

Gerstengarbe FW, Werner PC (1999) Estimation of the beginning and end of recurrent events within a climate regime. Climate Res 11: 97–107

Gong DY, Ho CH (2002) Shift in the summer rainfall over the Yangtze River valley in the late 1970s. Geophys Res Lett 29: 1436, doi: 10.1029/2001GL014523

Grinsted A, Moore JC, Jevrejeva S (2004) Application of the cross wavelet transform and wavelet coherence to geophysical time series. Nonlinear Proc Geophy 11: 561–566

Haan CT (2002) Statistical methods in hydrology (second Ed.). Blackwell, Iowa State Press

Helsel DR, Hirsch RM (1992) Statistical methods in water resources. Studies in Environmental Science. Elsevier, Amsterdam, 522 pp

Huang R, Zhang R, Zhang Q (2000) The 1997/98 ENSO cycle and its impact on summer climate anomalies in East Asia. Adv Atmos Sci 17: 348–362

IPCC (2007) Climate change 2007: The Physical Science Basis. In: Solomon S, Qin D, Manning M, Chen Z, Marquis M, Averyt KB, Tanor M, Miller HL (eds) Working Group I Contribution to the Intergovernmental Panel on Climate Change Fourth Assessment Report. Cambridge University Press, Cambridge, UK, p 996

Kendall MG (1975) Rank correlation methods. Griffin, London, UK

Kim KY, Wu QG (1999) A comparison study of EOF techniques: analysis of nonstationary data with periodic statistics. J Climate 12: 185–199

Labat D, Goddéris Y, Probst JL, Guyot JL (2004) Evidence for global runoff increase related to climate warming. Adv Water Resour 27: 631–642

Lana X, Serra C, Burgueño A (2001) Patterns of monthly rainfall shortage and excess in terms of the standardized precipitation index for Catalonia (NE Spain). Int J Climatol 21: 1669–1691

Liu B, Xu M, Henderson M, Qi Y (2005) Observed trends of precipitation amount, frequency, and intensity in China, 1960–2000. J Geophys Res 110: D08103, doi: 10.1029/2004JD004864

Loukas A, Vasiliades L, Dalezios NR (2002) Potential climate change impacts on flood producing mechanisms in southern British Columbia, Canada using the CGCMA1 simulation results. J Hydrol 259: 163–188

Mann HB (1945) Nonparametric tests against trend. Econometrica 13: 245–259

Mitchell JM, Dzerdzeevskii B, Flohn H, Hofmeyr WL, Lamb HH, Rao KN, Wallén CC (1966) Climate change, WMO Technical Note No. 79, World Meteorological Organization, 79 pp

Montroy DL (1997) Linear relation of central and eastern North American precipitation to tropical Pacific sea surface temperature anomalies. J Climate 10: 541–558

Qian W, Kang HS, Lee DK (2002) Distribution of seasonal rainfall in the East Asian monsoon region. Theor Appl Climatol 71: 151–168

Ren GY, Wu H, Chen ZH (2000) Spatial patterns of change trend in rainfall of China. Quart J Appl Meteor 11(3): 322–330 (in Chinese)

Richman MB (1986) Rotation of principal components. J Climatol 6: 293–335

Serrano VL, Mateos VL, García JA (1999) Trend analysis of monthly precipitation over the Iberian Peninsula for the period 1921–1995. Phys Chem Earth (B) 24(2): 85–90

Simmons AJ, Branstator GW, Wallace JM (1983) Barotropic wave propagation, instability and atmospheric teleconnection patterns. J Atmos Sci 40: 1363–1392

Torrence C, Compo GP (1998) A practical guide to wavelet analysis. Bull Amer Meteor Soc 79: 61–78

von Storch VH (1995) Misuses of statistical analysis in climate research. In: Storch HV, Navarra A (eds) Analysis of climate variability: application of statistical techniques. Berlin, Springer, pp 11–26

Wang HJ (2001) The weakening of the Asian Monsoon circulation after the end of the 1970s. Adv Atmos Sci 18: 376–386

Wang SW, Zhu JH, Cai JN (2004) Interdecadal variability of temperature and precipitation in China since 1880. Adv Atmos Sci 21: 307–313

Wang SY, Mcgrath R, Semmler T, Sweeney C (2006) Validation of simulated precipitation patterns over Ireland for the period 1961–2000. Int J Climatol 26: 251–266

Webster PJ, Magana VO, Palmer TN, Shukla J, Tomas RA, Yanai M, Yasunari T (1998) Monsoons: processes, predictability, and the prospects for prediction. J Geophys Res 103: 14451–14510

Xu C-Y, Singh VP (2004) Review on regional water resources assessment models under stationary and changing climate. Water Resour Manag 18: 591–612

Yang FL, Lau KM (2004) Trend and variability of China precipitation in spring and summer: linkage to sea-surface temperatures. Int J Climatol 24: 1625–1644

Yatagai A, Yasunari T (1995) Interannal variations of summer precipitation in the arid/semi-arid regions in China and Mongolia: Their regionality and relation to the Asian summer monsoon. J Meteor Soc Jpn 73: 909–923

Yue S, Wang CY (2004) The Mann-Kendall test modified by effective sample size to detect trend in serially correlated hydrological series. Water Resour Manag 18: 201–218

Yue S, Pilon P, Phinney B, Cavadias G (2002) The influence of autocorrelation on the ability to detect trend in hydrological series. Hydrol Process 16: 1807–1829

Zhai PM, Sun A, Ren F, Liu X, Gao B, Zhang Q (1999a) Changes of climate extremes in China. Clim Change 42: 203–218

Zhai PM, Ren FM, Zhang Q (1999b) Detection of trends in China's precipitation extremes. Acta Meteor Sinica 57: 208–216 (in Chinese)

Zhai PM, Zhang XB, Wan H, Pan XH (2005) Trends in total precipitation and frequency of daily precipitation extremes over China. J Climate 18: 1096–1108

Zhang Q, Gemmer M, Chen JQ (2007) Flood/drought changes during past 1000 years in the Yangtze Delta region and possible connections with Tibetan climatic changes. Global Planet Change 57: 213–221

Zhang Q, Liu CL, Xu C-Y, Xu Y-P, Jiang T (2006a) Observed trends of annual maximum water level and streamflow during past 130 years in the Yangtze River basin, China. J Hydrol 324: 255–265

Zhang Q, Xu C-Y, Becker S, Jiang T (2006b) Sediment and runoff changes in the Yangtze River basin during past 50 years. J Hydrol 331: 511–523

Zhao ZG, Xu L (2002) Potential impact on El Niño events on the circulation and climate variation in China. Wea Climate 1: 109–118